Transfer matrix study of the chiral clock model in the Hamiltonian limit

1989 J. Phys. A: Math. Gen. 22 2475

(http://iopscience.iop.org/0305-4470/22/13/040)

J. Phys. A: Math. Gen. **22** (1989) 2475–2494. Printed in the UK

Transfer matrix study of the chiral clock model in the Hamiltonian limit

H U Everts and H Röder

Institut für Theoretische Physik, Universität Hannover, Appelstrasse 2, D-3000 Hannover, Federal Republic of Germany

Received 25 July 1988, in final form 3 January 1989

Abstract. The logarithm of the transfer matrix of the two-dimensional, three-state chiral clock model is shown to be equivalent to a one-dimensional non-Hermitian quantum Hamiltonian. In the region of small chirality the critical behaviour of the quantum model is investigated by a series expansion and by finite-size scaling. A single phase boundary between a modulated paramagnetic and a ferromagnetic phase is located with good accuracy. Both methods yield comparable results for the critical exponent $\bar{\beta}$ of the wavevector of the modulated high-temperature phase. The critical exponents ν_x, ν_τ for the correlation lengths obtained from finite-size scaling point towards the existence of a Lifshitz point at finite chirality. The results of the series expansion for the exponent ν_x, however, are inconsistent with finite-size scaling. For larger chirality our finite-size results clearly reveal the occurrence of an incommensurate phase with algebraically decaying correlations between the ferromagnetic and the modulated paramagnetic phase. We analyse the critical behaviour of this incommensurate phase at its melting line and determine the exponent η that controls the algebraic decay of correlations.

1. Introduction

Layers of adsorbed gases on crystalline substrates may exhibit commensurate and incommensurate ordered phases in the submonolayer regime. A well known example is the system H/Fe(001) which for a certain coverage forms an ordered commensurate (3×1) phase while the high-temperature phase is in an incommensurate fluid state (e.g. Imbihl *et al* 1982). Simple considerations of the interface energies of walls between the three possible domains of the (3×1) structure have led to the conclusion that the appropriate Landau–Ginzburg–Wilson Hamiltonian must contain a uniaxial chiral term (Huse and Fisher 1982, 1984). The simplest lattice model that incorporates such a term is the three-state chiral clock (CC3) model (Huse 1981, Ostlund 1981). Its phase diagram is shown schematically in figure 1(*a*). It is well established that for sufficiently large chirality an incommensurate floating phase, i.e. a phase with algebraically decaying order parameter correlations, occurs between the ordered commensurate and the incommensurate fluid phase (Ostlund 1981, Centen *et al* 1982, Selke and Yeomans 1982, Haldane *et al* 1983, Houlrik *et al* 1983, Howes 1983, Schulz 1980, 1983, Duxbury *et al* 1984). The question, however, of whether the Lifshitz point (Δ_L, T_L), at which the floating phase ends, lies at a finite value of the chirality parameter Δ as suggested in figure 1(*a*) or whether the floating phase extends to zero chirality remains controversial. Of the above-quoted authors Haldane *et al* (1983) and Schulz (1983) predicted the

0305-4470/89/132475+20$02.50

floating phase to intervene between the commensurate and the incommensurate phases for all values of Δ, i.e. $\Delta_L = 0$. The others suggest values of Δ_L in the range $0.3 \leq \Delta_L \leq 0.4$. Apart from this controversy over a qualitative feature of the phase diagram of the CC3 model there are uncertainties concerning the critical properties at the various phase boundaries. Among the authors who agree on the existence of a Lifshitz point at finite Δ, there is no agreement about the nature of the transition from the ordered to the incommensurate disordered state. According to Howes (1983) the transition is in the Potts universality class; Huse and Fisher (1982, 1984) propose that it should be in a new chiral universality class and their conjecture is supported by numerical work of Duxbury *et al* (1984), but is questioned by recent work of Vescan *et al* (1986).

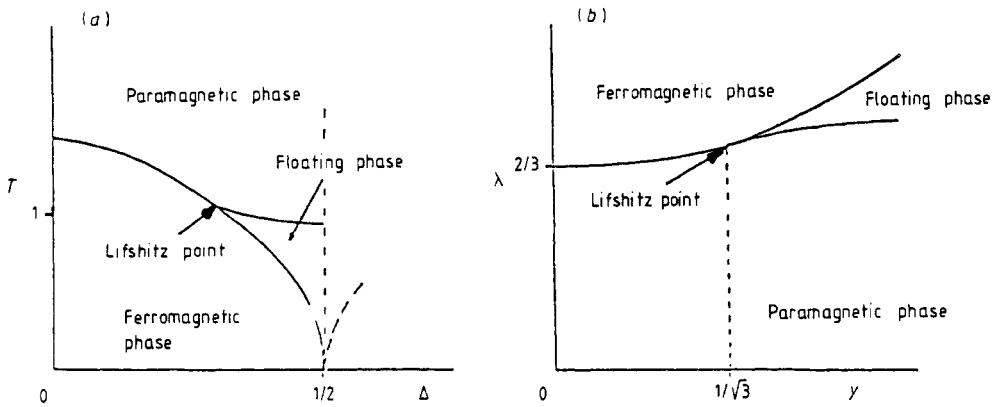

Figure 1. Phase diagrams of (*a*) the CC3 lattice model and (*b*) the Hamiltonian (2.4).

Most of the above approaches that have led to the conflicting results about the disordered to commensurate transition yield no information about the nature of the incommensurate floating phase. The properties of this phase have, in the main, been deduced from a low-temperature free fermion approximation (Ostlund 1981, Haldane *et al* 1983). Within this approximation the array of parallel domain walls that constitute the incommensurate phase is assumed to be almost free of dislocations. As a result the floating phase should bear the characteristics of a Kosterlitz–Thouless (KT) phase (Kosterlitz and Thouless 1973, Kosterlitz 1974). In particular the exponent η that determines the spatial decay of the correlations should be non-universal $\eta = \eta(T, \Delta)$. The melting of the floating phase should happen via a KT transition at $\eta(T, \Delta) = 1/4$ (Ostlund 1981, Haldane *et al* 1983). The last assertion depends on the assumption that the dislocation density of the domain wall array is still low even at the melting temperature. This has never been checked in an independent calculation. In previous numerical analyses of the CC3 model (Selke and Yeomans 1982, Duxbury *et al* 1984) no attempt has been made to determine η, so it remains an open question whether the melting of the floating phase does occur via a KT transition.

In the present paper we consider the transfer matrix of the CC3 model in the Hamiltonian limit. In two dimensions the classical action of the more general p-state model is given by

$$A^{(p)}(K_x, K_\tau, \Delta) = -\sum_{\boldsymbol{R}} \left[K_x \cos\left(\frac{2\pi}{p}(n_{\boldsymbol{R}+\boldsymbol{x}} - n_{\boldsymbol{R}})\right) + K_\tau \cos\left(\frac{2\pi}{p}(n_{\boldsymbol{R}+\boldsymbol{\tau}} - n_{\boldsymbol{R}} + \Delta)\right)\right] \tag{1.1}$$

where $\boldsymbol{R} = (R_\tau, R_x)$ denotes a point on the square lattice (figure 2) and $\boldsymbol{x}$, $\boldsymbol{\tau}$ are the primitive lattice vectors, $|\boldsymbol{x}| = a_x$, $|\boldsymbol{\tau}| = a_\tau$. Without loss of generality (Ostlund 1981) we assume the interaction parameters K_x, K_τ to be positive and the chirality parameter Δ to be in the range $0 \leq \Delta \leq \frac{1}{2}$. The variables $n_{\boldsymbol{R}}$ which take the values $0, 1, \ldots, p$ define the local spin variables

$$\boldsymbol{S}(\boldsymbol{R}) = \left(\cos\left(\frac{2\pi}{p} n_{\boldsymbol{R}}\right), \sin\left(\frac{2\pi}{p} n_{\boldsymbol{R}}\right)\right). \tag{1.2}$$

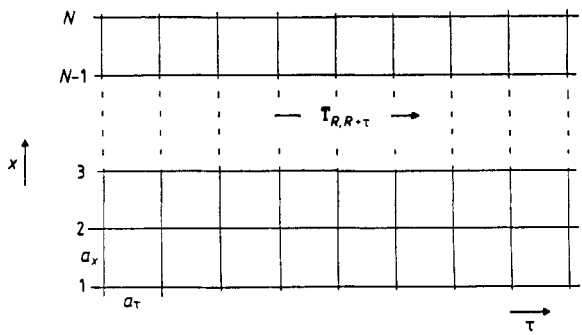

Figure 2. Description of the lattice which is used for setting up the transfer matrix.

The two-spin correlation function of the model is of the general form

$$\langle \boldsymbol{S}(\boldsymbol{R})\boldsymbol{S}(0)\rangle \sim \frac{A}{R^\eta} \cos(QR_\tau) \exp\left(-\frac{R_\tau}{\xi_\tau} - \frac{R_x}{\xi_x}\right) + \boldsymbol{M}^2 \tag{1.3}$$

where $\boldsymbol{M}$ is the ferromagnetic order parameter. The modulation along the τ direction is induced by the chirality Δ. One expects the wavenumber Q to be proportional to Δ at high temperatures. The correlation lengths along the two lattice directions, ξ_x and ξ_τ, will in general be different; previous investigators (Duxbury *et al* 1984, Vescan *et al* 1986) claim that there may even be anisotropic scaling in certain regions of the transition lines in figure 1(*a*).

We consider the column-to-column transfer matrix $\mathbf{T}_{R,R+\tau}$ (see figure 2). Its eigenvalues will in general be complex. The correlation length ξ_τ and the wavenumber Q of the correlation function (1.3) are related to the real and imaginary parts of the largest and the second-largest eigenvalue of the transfer matrix.

It is known (Kogut 1979) that the transfer matrix can be represented as

$$\mathbf{T}_{R,R+\tau} = [\mathrm{e}^{-\gamma H}]_{R,R+\tau} \tag{1.4}$$

where γ is a constant and H is a one-dimensional quantum Hamiltonian. ξ_τ and Q can be obtained from the eigenvalues of H with the minimal and next to minimal real

parts. The derivation of the proper quantum Hamiltonian for the CC3 model will be discussed in §2 of the paper. In §3 the critical exponents of Q and ξ_τ are presented as results of a series expansion for the appropriate eigenvalues of H. Section 4 contains a finite-size analysis of these eigenvalues. We determine the critical exponents of Q and ξ_x and, in addition, the anisotropy parameter (Kinzel and Yeomans 1981, Schaub and Domany 1983, Domany and Schaub 1984). In the low-chirality region this analysis allows a check on the results of the series expansion. For higher chirality we obtain the critical exponents that govern the incommensurate to commensurate transition and the melting transition of the floating phase. We observe that in a certain region of the phase diagram scaling is isotropic, i.e. $\xi_x \sim \xi_\tau \sim N$, so that using a proper redefinition of the spin variables $S(\boldsymbol{R})$, (1.2), the correlation function (1.3) can be cast in a conformally invariant form (§5). Exploiting the consequences of conformal invariance we then determine numerically the critical exponent η. In §6 we summarise and discuss the main results.

2. The quantum Hamiltonian

Various methods which lead to the formulation (1.4) of the transfer matrix have been proposed in the literature (Hamer *et al* 1979, Kogut 1979). Here we shall briefly discuss two of them.

(i) Following Kogut (1979), Marcu *et al* (1981) derive the quantum Hamiltonian by taking the limit $K_x \to 0$, $K_\tau \to \infty$ such that $K_x \exp\{K_\tau[\cos\frac{2}{3}\pi\Delta - \cos\frac{2}{3}\pi(\Delta+1)]\}$ remains fixed. In this limit the only non-negligible elements of $\mathbf{T}_{\boldsymbol{R},\boldsymbol{R}+\boldsymbol{\tau}}$ are those corresponding to

$$n_{\boldsymbol{R}+\boldsymbol{\tau}} = n_{\boldsymbol{R}} \qquad R_x = 1,\ldots,N \qquad \text{(no spin flip)} \tag{2.1a}$$

and to

$$n_{\boldsymbol{R}_j+\boldsymbol{\tau}} = n_{\boldsymbol{R}_j} + 1 \qquad \text{or} \qquad n_{\boldsymbol{R}_j+\boldsymbol{\tau}} = n_{\boldsymbol{R}_j} + 2 \qquad R_{x_j} = ja_x$$
$$\text{and} \tag{2.1b}$$
$$n_{\boldsymbol{R}+\boldsymbol{\tau}} = n_{\boldsymbol{R}} \qquad \boldsymbol{R} \neq \boldsymbol{R}_j \qquad j = 1,\ldots,N.$$

In the last two cases a single spin in the column $\boldsymbol{R}+\boldsymbol{\tau}$ deviates by one or two units from the adjacent spin in column $\boldsymbol{R}$. The corresponding matrix elements are

$$\exp\{K_\tau[\tfrac{3}{2}\cos(\tfrac{2}{3}\pi\Delta) \pm \tfrac{1}{2}\sqrt{3}\sin(\tfrac{2}{3}\pi\Delta)]\}. \tag{2.1c}$$

Of these Marcu *et al* (1981) retain only the larger one as they consider the limit $K_\tau \to \infty$ at a fixed value of Δ. In contrast we take the combined limit $K_x \to 0$, $K_\tau \to \infty$, $\Delta \to 0$ and require that the parameters

$$\tilde{K}_\tau = \tfrac{1}{2}\sqrt{3}K_\tau \sin(\tfrac{2}{3}\pi\Delta) \tag{2.2}$$

and

$$\lambda = K_x \frac{\exp[K_\tau \tfrac{3}{2}\cos(\tfrac{2}{3}\pi\Delta)]}{\cosh \tilde{K}_\tau} \tag{2.3}$$

remain fixed. Following the derivation of Marcu *et al* (1981) we then arrive at an expression of the type (1.4) for the transfer matrix where

$$H(\lambda, y) = \sum_{j=1}^{N} \left(\frac{2}{3} - \frac{1}{3}(\sigma_j + \sigma_j^+) + \frac{1}{\sqrt{3}} y(\sigma_j - \sigma_j^+) - \frac{\lambda}{2}(\Gamma_j \Gamma_{j+1}^+ + \text{HC}) \right) \tag{2.4}$$

with

$$y = \frac{1}{\sqrt{3}} \tanh \tilde{K}_\tau \tag{2.5}$$

and

$$\sigma = \begin{pmatrix} 1 & 0 & 0 \\ 0 & \exp(\frac{2}{3}\pi \mathrm{i}) & 0 \\ 0 & 0 & \exp(-\frac{2}{3}\pi \mathrm{i}) \end{pmatrix} \qquad \Gamma = \begin{pmatrix} 0 & 1 & 0 \\ 0 & 0 & 1 \\ 1 & 0 & 0 \end{pmatrix}. \tag{2.6}$$

For the constant γ in (1.4) we find $\gamma = 3\lambda/2K_x$. The Hamiltonian obtained by Marcu *et al* (1981) follows from (2.4) in the limit $\tilde{K}_\tau \to \infty$, i.e. $y \to 1/\sqrt{3}$. For this case the model has been investigated by Vescan *et al* (1986). In the numerical analysis (see §4) it turned out to be convenient to work with the Hamiltonian

$$H' = H/\sqrt{1+y^2} = \sum_{j=1}^{N} \left(\Omega_j - \frac{\lambda'}{2} (\Gamma_j \Gamma_{j+1}^+ + \text{HC}) \right) \tag{2.7a}$$

where

$$\Omega_j = \begin{pmatrix} 0 & 0 & 0 \\ 0 & \exp(\mathrm{i}\psi) & 0 \\ 0 & 0 & \exp(-\mathrm{i}\psi) \end{pmatrix} \tag{2.7b}$$

with

$$\psi = \tan^{-1} y \tag{2.7c}$$

and

$$\lambda' = \lambda/\sqrt{1+y^2} = \lambda \cos \psi. \tag{2.7d}$$

(ii) A second approach to (1.4) starts from the observation that the original classical action $A^{(p)}$, (1.1), may be considered as the Euclidean action of a two-dimensional quantum field theory on a lattice with the field variables $\theta(\boldsymbol{R}) = (2\pi/p)n_{\boldsymbol{R}}$. Taking the continuum limit in the τ direction the respective interaction term in (1.1) may be expanded for large p:

$$\cos\left(\frac{2\pi}{p}(n_{\boldsymbol{R}+\tau} - n_{\boldsymbol{R}} + \Delta) \right) \simeq 1 - a_\tau \hat{\partial}_\tau \theta \sin(2\pi\Delta/p) - \tfrac{1}{2} a_\tau^2 \hat{\partial}_\tau^2 \theta \cos(2\pi\Delta/p). \tag{2.8}$$

Proceeding as in the case of the O(2) symmetric model (see Hamer *et al* 1979) one then arrives at the following Hamiltonian in the limit of large p:

$$H_{p\to\infty} = \frac{1}{a_\tau K_\tau \cos(2\pi\Delta/p)} \sum_{R_x=1}^{N} \{ \tfrac{1}{2} L^2(R_x) + \mathrm{i} K_\tau L(R_x) \sin(2\pi\Delta/p) - K_x K_\tau \cos(2\pi\Delta/p) \cos[\theta(R_x + x) - \theta(R_x)] \}. \tag{2.9}$$

$L(R_x)$ is the angular momentum operator conjugate to $\theta(R_x)$. We return to finite p by replacing (Elizur *et al* 1979)

$$L^2 \to \frac{1-\cos(L_p)}{1-\cos(2\pi/p)} \qquad L \to \frac{\sin(L_p)}{\sin(2\pi/p)} \tag{2.10a}$$

and

$$\theta \to \theta_p \tag{2.10b}$$

where

$$[L_p(R_x), \theta_p(R'_x)] = -(2i\pi/p)\delta_{R_x,R'_\tau}. \tag{2.11}$$

Both L_p and θ_p have the spectrum $(2\pi/p)Z_p$ where Z_p are the integers modulo p. For $p = 3$ we then recover the Hamiltonian (2.4). However, the relationship between the coupling constants K_x, K_τ and the parameters λ and y is different from (2.2) and (2.3):

$$\lambda = K_x K_\tau \cos(\tfrac{2}{3}\pi\Delta) \qquad y = K_\tau \sin(\tfrac{2}{3}\pi\Delta). \tag{2.12}$$

In the above derivation we have not established (1.4) exactly but rather

$$T^{N_\tau} = \text{constant} \times \exp(-N_\tau \gamma H) \tag{2.13}$$

where $N_\tau = 1/a_\tau$ is the number of 'time slices' into which the unit interval in the τ direction has been divided. Thus we have

$$\gamma = [K_\tau \cos(\tfrac{2}{3}\pi\Delta)]^{-1}. \tag{2.14}$$

There is an obvious qualitative difference between the assignments of the coupling constants K_x, K_τ, Δ of $A^{(3)}$ to the parameters λ, y of the Hamiltonian H following from the different derivations (i) and (ii). While y is found to be unbounded from (ii), one has $0 \le y \le 1/\sqrt{3}$ according to (i). The limit $K_x \to 0$ which has to be performed in (i) invalidates the free fermion approximation by which the existence of an incommensurate floating phase in the CC3 model is established (Ostlund 1981, Centen *et al* 1982). Clearly, the picture of an array of domain walls running mostly parallel to the x direction so that only a few of the ferromagnetic K_x bonds are broken does not apply for $K_x \to 0$. Thus we do not expect to find a massless phase in the Hamiltonian (2.4) in the parameter range $0 \le y \le 1/\sqrt{3}$, where H can be derived from the exact transfer matrix by procedure (i). On the other hand, the quantum model defined by H belongs to the same universality class as the original classical model. The spectrum of H must therefore reflect the entire phase diagram of the CC3 model including the floating phase. These arguments suggest that a Lifshitz point will be located at a value $y_L \ge 1/\sqrt{3}$ in the quantum model and that the spectrum of H is massless in an interval $\lambda_c^{KT} < \lambda < \lambda_c^{ferro}$ between the ferromagnetic and the disordered phase for $y > y_L$.

A few structural properties of the spectrum of H follow directly from symmetries. The Z_3 charge

$$\tilde{q} = \sum_{j=1}^{N} \tilde{q}_j (\text{mod } 3) \tag{2.15}$$

where

$$\tilde{q}_j = \begin{pmatrix} 0 & 0 & 0 \\ 0 & 1 & 0 \\ 0 & 0 & 2 \end{pmatrix}_j \tag{2.16}$$

in a basis in which the matrices σ_j are diagonal (σ basis), is a conserved quantity. The eigenvalues belonging to the three sectors $\tilde{q} = 0, 1, 2$ will be denoted by $\Lambda_N^{(\tilde{q})}$ for a chain of N members. We shall exclusively deal with periodic boundary conditions so that the eigenvalues can be labelled by the wavenumber $k = 2\pi n/N$, $n = 0, 1, \ldots, N-1$. For physical reasons the ground-state energy $\Lambda_N^{(0)}(0)$ is real. Furthermore, since H is parity conserving

$$\Lambda_N^{(1)}(k) = [\Lambda_N^{(2)}(k)]^* \tag{2.17}$$

and since states with fewer nodes are lower in energy

$$\mathrm{Re}\{\Lambda_N^{(m)}(0)\} \leq \mathrm{Re}\{\Lambda_N^{(m)}(k>0)\} \qquad m = 0, 1, 2. \tag{2.18}$$

The correlation length ξ_τ and the wavenumber Q which give the asymptotics of the correlation function (1.3) at large R_τ are related to the mass gap G of H and to $\mathrm{Im}\{\Lambda_N^{(1)}(0)\}$:

$$\xi_\tau^{-1} = G = \lim_{N\to\infty} G_N = \lim_{N\to\infty} [\mathrm{Re}\{\Lambda_N^{(1)}(0)\} - \Lambda_N^{(0)}(0)] \tag{2.19}$$

$$Q = \lim_{N\to\infty} Q_N = \lim_{N\to\infty} [\mathrm{Im}\{\Lambda_N^{(1)}(0)\}]. \tag{2.20}$$

It is clear that Q will primarily depend on the parameter y which multiplies the non-Hermitian part of the Hamiltonian (2.4). As $y \to \infty$, Q will grow to infinity for any finite value of λ. For the original lattice model Q attains its maximum value at $\Delta = \frac{1}{2}$. Thus in the y–λ plane the phase diagram will differ from figure 1(a) in as much as the critical point $\Delta = \frac{1}{2}$, $K_x = 0$ is shifted to infinity (see figure 1(b)).

Let us mention that for $y = 0$ the Hamiltonian (2.4) represents the three-state Potts model. $H(0, \lambda)$ is self-dual with respect to $\lambda = \frac{2}{3}$ (Elizur *et al* 1979).

It should be mentioned that a different Hamiltonian representation of the CC3 model is obtained if one starts with the row-to-row transfer matrix $\mathbf{T}_{R,R+x}$ (Centen *et al* 1982, Howes 1983). For $y = 0$, i.e. for the symmetric Potts model, the two Hamiltonians are identical.

3. Series analysis

The difference

$$\Lambda^{(1)}(0) - \Lambda^{(0)}(0) = G + \mathrm{i}Q \tag{3.1}$$

may be calculated perturbatively as a power series in λ. Note that for both assignments of λ to the interaction parameters of the original CC3 model obtained in §2, $\lambda \to 0$ as

$K_x \to 0$. Hence the expansion in powers of λ is a high-temperature expansion. The coefficients of the series

$$G(\lambda, y) = \sum_{n=0}^{\infty} a_n(y)\lambda^n \tag{3.2}$$

$$Q(\lambda, y) = y \sum_{n=0}^{\infty} b_n(y)\lambda^n \tag{3.3}$$

were obtained by the connected-diagram perturbation method of Kadanoff and Kohmoto (1981). This method was originally devised for the calculation of the ground-state energy of a Hermitian many-particle Hamiltonian. Its application to the present case of a non-Hermitian Hamiltonian is straightforward. Since the eigenstates that correspond to $\Lambda^{(0)}(0)$ and $\Lambda^{(1)}(0)$ belong to different charge sectors they can be treated as ground states in the respective sectors. The coefficients $a_n(y)$, $b_n(y)$, $n = 0, \ldots, 7$ are rational functions of y^2 which are too extensive for publication but can be supplied on request. For the Potts model (y=0) the coefficients $a_n(0)$ can be found in the work of Elizur *et al* (1979). In this case the analysis of the series is greatly facilitated by the fact that it is known to have a singularity at the self-dual point $\lambda_{sd} = \frac{2}{3}$. We calculated the [4/2], [3/3] and [2/4] Padé approximants to the logarithmic derivatives (dlog Padé approximants) of the series (3.2) for the mass gap for various values of y. From these we were able to locate the physical singularity $\lambda_c(y)$ corresponding to a phase transition by assuming that it evolves smoothly from λ_{sd} as y is increased. The Padé approximants always contained unphysical singularities in the complex λ plane. We employed an Euler transformation

$$u = \frac{1}{1 + \lambda b} \tag{3.4}$$

to shift them to a distance larger than $u_c = (1 + b\lambda_c)^{-1}$ from the origin. Tables 1 and 2 show the results as obtained from the [4/2], [3/3] and [2/4] dlog Padé approximants to the Euler transformed series (3.2) in the range $0 \leq y \leq 2$. λ_c is the critical coupling and ν_τ the critical exponent of the correlation length ξ_τ, $\xi_\tau = G^{-1} \simeq (\lambda_c - \lambda)^{-\nu_\tau}$. While the [4/2] approximant behaves sometimes irregularly—in one case it does not even exhibit a physical pole—the poles of the other two approximants are consistent with each other: three of the poles of the [2/4] approximant lie close to the poles of the [3/3] approximant; the additional pole lies on the real λ axis at a larger distance from the origin than λ_c.

The dlog Padé approximants to the series (3.3) for the wavenumber Q exhibit an unphysical pole on the negative λ axis which is closer to the origin than the physical pole and has a residue nearly twice as large as that of the physical pole. This behaviour makes it impossible to reliably determine the critical coupling λ_c^{ferro} (where Q vanishes) from these approximants. Adopting a result of the finite-size analysis (see §4) we set $\lambda_c^{\text{ferro}} = \lambda_c$, i.e. we identified the critical couplings of the mass gap and of the wavenumber, and calculated the dlog Padé approximants for the series

$$(\lambda - \lambda_c)Q(\lambda, y) = y(\lambda - \lambda_c) \sum_{n=0}^{7} b_n(y)\lambda^n \tag{3.5}$$

Table 1. Positions of the poles of the respective dlog Padé approximants to the high-temperature series. These are approximants to the critical coupling λ_c.

ψ	y	[4,2]	[3,3]	[2,4]
0.0000	0.0000	0.6594	0.6667	0.6691
0.1500	0.1511	0.71[a]	0.6867	0.6874
0.3000	0.3093	—[b]	0.7353	0.7359
0.4500	0.4830	0.8014	0.8185	0.8186
0.5236	$1/\sqrt{3}$	0.8491	0.8713	0.8723
0.5764	0.6500	0.8602	0.9166	0.9176
0.6435	0.7500	0.9110	0.9839	0.9843
0.6747	0.8000	0.9352	1.019	1.019
0.7045	0.8500	0.9595	1.055	1.056

[a] Intervening non-physical zero on the negative λ axis around -0.345.
[b] Only two complex conjugated roots exist.

Table 2. Residues of the respective dlog Padé approximants at the pole positions of table 1. These are approximants to the correlation length exponent ν_τ.

ψ	y	[4,2]	[3,3]	[2,4]
0.0000	0.0000	0.7936	0.8380	0.8500
0.1500	0.1511	1.0[a]	0.8456	0.8564
0.3000	0.3093	—[b]	0.8292	0.8313
0.4500	0.4830	0.7610	0.8437	0.8478
0.5236	$1/\sqrt{3}$	0.7573	0.8733	0.8743
0.5764	0.6500	0.6251	0.8989	0.9039
0.6435	0.7500	0.6111	0.9554	0.9574
0.6747	0.8000	0.5983	0.9887	0.9894
0.7045	0.8500	0.5851	1.024	1.025

[a] Intervening non-physical zero on the negative λ axis around -0.345.
[b] Only two complex conjugated roots exist.

at $\lambda = \lambda_c$. From these we were able to extract the critical exponent $\bar{\beta}$ which describes how the wavenumber goes to zero as λ approaches λ_c from below:

$$Q \simeq (\lambda_c - \lambda)^{\bar{\beta}} \qquad \lambda < \lambda_c \tag{3.6}$$

The results are listed in table 3. We note that for a Pokrovsky–Talapov-type incommensurate to commensurate transition $\bar{\beta}$ should take the value $\frac{1}{2}$ (Pokrovsky and Talapov 1978, 1980).

Presumably all of the above results become less and less reliable as y increases, because then the critical coupling λ_c increases beyond unity while the original expansion was around $\lambda = 0$. Nevertheless we think it remarkable that the two critical indices ν_τ and $\bar{\beta}$ turn out to be different for all values of y. This contradicts the previous finding (Duxbury *et al* 1984) that the transition between the ferromagnetic and the incommensurate disordered state should be a chiral transition (Huse and Fisher 1982, 1984). There is no direct sign of a Lifshitz point or for the existence of an incommensurate floating phase in our series results. We think, however, that the decrease of $\bar{\beta}$ towards the Pokrovsky–Talapov value $\bar{\beta} = 0.5$ (Pokrovsky and Talapov 1978, 1980) as y increases to $y \simeq 0.8$ (see table 3) is a hint for a Lifshitz point around $y \simeq 0.8$.

Table 3. Values of the respective dlog Padé approximants to the high-temperature series taken at the estimates λ_c^* for the critical coupling. These are approximants to the wavenumber exponent $\overline{\beta}$. The entry for $y = 0$, where $Q = 0$, reflects a singularity in Q/y (see formula (3.3)).

ψ	y	[4,2]	[3,3]	[2,4]	λ_c^*
0.0000	0.0000	0.7000	0.7019	0.7293	2/3
0.1500	0.1511	0.6821	0.6876	0.7099	0.687
0.3000	0.3093	0.85[a]	0.6230	0.6420	0.736
0.4500	0.4830	0.6145	0.5759	0.5955	0.819
0.5236	$1/\sqrt{3}$	0.5959	0.5617	0.5823	0.872
0.5764	0.6500	0.5864	0.5555	0.5770	0.917
0.6435	0.7500	0.5821	0.5545	0.5801	0.984
0.6747	0.8000	0.5829	0.5483	0.5843	1.02
0.7045	0.8500	0.5880	0.6346	0.5920	1.06

[a] Zero on the negative λ axis with large residuum.

4. Finite-size scaling analysis

4.1. Paramagnetic to commensurate transition

Another method of obtaining the correlation length ξ_τ and the wavenumber Q is to numerically diagonalise the Hamiltonian (2.4) for finite chain lengths. The critical properties can then be estimated with the use of finite-size scaling (see e.g. Nightingale 1976, Barber 1983).

The sizes of the matrices which have to be diagonalised increases rapidly as 3^N with the chain length N. We therefore utilised all possible symmetries (translational invariance, Z_3 charge conservation) to block-diagonalise the Hamiltonian. Even so, in order to be able to scan reliably through a two-dimensional parameter space we had to modify a Lanczos method for complex symmetric matrices (Lanczos 1950, Paige 1972, Cullum and Willoughby 1985, 1986) to be able to go to chain lengths of $N = 10$. The computational effort, however, was greatly facilitated by the fact that the desired eigenvalues $\Lambda_N^{(0)}(0)$ and $\Lambda_N^{(1)}(0)$ happen to lie on the very edge of the eigenvalue spectrum of the respective block. This means that these are the eigenvalues for which the above-mentioned diagonalisation procedure is supposed to converge fastest (see Cullum and Willoughby 1986).The block diagonalisation of the $N = 10$ chain took around 80 000 CPU seconds on a Cyber 990. After this had been done, however, obtaining an eigenvalue for the $N = 10$ chain was done in only about 300 CPU seconds.

As usual in finite-size scaling techniques we use the relation

$$\xi_{\tau N}^{-1} = G_N(\lambda) = N^{-\Theta^{(1)}} F(N^{1/\nu_\tau}\tilde{\lambda}) \qquad \tilde{\lambda} = \lambda_c - \lambda \qquad \Theta^{(1)} = \nu_\tau/\nu_x \tag{4.1}$$

to obtain estimates for the finite-size critical points λ_{cN} and the correlation length exponents ν_τ and ν_x. A value of $\Theta^{(1)} \neq 1$ indicates anisotropic scaling (Domany and Schaub 1984). In the case of a modulated system one expects the wavevector Q to suffice a similar scaling relation

$$Q_N(\lambda) \simeq N^{-\Theta^{(2)}} H(N^{1/\nu_x'}\hat{\lambda}) \qquad \hat{\lambda} = \lambda_c^{\text{ferro}} - \lambda \qquad \Theta^{(2)} = \overline{\beta}/\nu_x' \tag{4.2}$$

describing how the wavevector goes to zero as the coupling constant approaches the ferromagnetic regime. In order to allow for anisotropic scaling we used the equations

$$Y_N(\lambda_{cN}) = Y_{N+1}(\lambda_{c_N}) = \Theta_N^{(1)} \tag{4.3}$$

and

$$K_N(\lambda_{cN}^{\text{ferro}}) = K_{N+1}(\lambda_{c_N}^{\text{ferro}}) = \Theta_N^{(2)} \tag{4.4}$$

where

$$Y_N = \frac{\log(G_N/G_{N+1})}{\log[(N+1)/N]} \qquad K_N = \frac{\log(Q_N/Q_{N+1})}{\log[(N+1)/N]} \tag{4.5}$$

to obtain finite-size estimates for the critical coupling of the correlation length λ_{cN} and for the critical coupling of the wavenumber $\lambda_{cN}^{\text{ferro}}$. These finite-size estimates were then extrapolated using the Van den Broeck–Schwartz (VBS) extrapolation technique (Van den Broeck and Schwartz 1979, Barber 1983) with a value of $\alpha_L = 1$ (for an example see table 4). Further information can be obtained from the critical exponents ν_x' and ν_x for which finite-size estimates were calculated through

$$1/\nu_{xN} = \tfrac{1}{2}(Z_N + Z_{N+1}) + \Theta_N^{(1)} \tag{4.6a}$$

with

$$Z_N = \frac{\log[(\mathrm{d}G_N/\mathrm{d}\lambda)/(\mathrm{d}G_{N+1}/\mathrm{d}\lambda)]}{\log[(N+1)/N]} \tag{4.6b}$$

and through a similar formula for ν_{xN}' in which $\mathrm{d}G_N/\mathrm{d}\lambda$ goes over into $\mathrm{d}Q_N/\mathrm{d}\lambda$ and $\Theta_N^{(1)}$ into $\Theta_N^{(2)}$. In contrast to the work by Vescan *et al* (1986) the quantities G_N, Q_N, Z_N and $\Theta_N^{(1,2)}$ were calculated at the extrapolated values of the bulk critical coupling λ_c and λ_c^{ferro} and not at the finite-size critical couplings. Both procedures give the same answer in the infinite-system limit, but the finite-size estimates for the exponents taken at the bulk critical coupling seem to behave more regularly.

Table 4. VBS table for $\Theta^{(1)}$ at a value of ψ=0.15. The finite-size estimates were taken at the extrapolated bulk critical coupling $\lambda_c = 0.6855$.

1.038 078 2			
1.016 422 3	0.991 319 44		
1.004 796 1	0.986 119 45	0.980 740 03	
0.997 630 55	0.983 039 30	0.979 447 37	0.978 818 63
0.992 824 93	0.981 168 48	0.978 967 91	
0.989 422 17	0.980 061 26		
0.986 926 58			

From plots of NG_N for various lattice sizes we deduce the existence of a conventional phase transition for values of y which are less than $1/\sqrt{3}$ with an anisotropy parameter of about one (see figure 3). Around $y = 1/\sqrt{3}$ a new structure begins to develop in the scaled mass gap NG_N (see figure 4(*a*)) which becomes more pronounced for larger values of y (see figures 4(*b*) and 4(*c*)). Similar structures have previously been

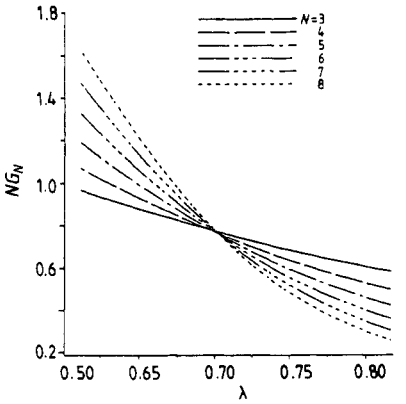

Figure 3. The scaled mass gap NG_N for y=0.2027 for lattice sizes $N = 3,\ldots,8$. The lines are interpolated between data points which were 0.015 units of the λ axis apart.

seen in the function Y_N for various models with competing interactions (Duxbury *et al* 1984, Domany and Schaub 1984, Beale *et al* 1985, Oitmaa *et al* 1987) and have been interpreted as evidence for the occurrence of an incommensurate floating phase in these models. The melting line of the floating phase was then analysed using conventional finite-size scaling, i.e. using (4.1) for the finite-size quantities. This procedure must fail if the melting transition of the floating phase is of the Kosterlitz–Thouless type with an essential singularity of $\xi_\tau(\tilde{\lambda})$ at $\tilde{\lambda} = 0$. An appropriate finite-size scaling analysis in this regime of the coupling constant will be given below.

The scaling of the wavevector Q is not expected to be influenced qualitatively by the existence of a floating phase and should therefore obey the scaling relation (4.2) in the whole range of the chirality parameter y. This works out well for small values of y (see figure 5) but for larger values of y an increasing even–odd asymmetry in the scaling function for finite lattices of length N renders a conventional finite-size analysis difficult. We therefore extrapolated the finite-size wavevectors Q_N to $Q_\infty(N)$ using the Bulirsch–Stoer (BS) algorithm (Bulirsch and Stoer 1964) and fitted these data to

$$Q_\infty \simeq (\lambda_c^{\text{ferro}} - \lambda)^{\bar{\beta}} \tag{4.7}$$

giving $\bar{\beta} = 0.5$ for both $y = 1.96$ and $y = 5.7979$.

Table 5. The extrapolated finite-size data following from the application of formulae (4.3), (4.5), (4.6*a*) and (4.6*b*). The system sizes considered were in the range $N = 3,\ldots,10$. The finite-size estimates for the exponents and $\Theta^{(1)}$ were calculated at the extrapolated critical coupling λ_c. The indicated errors arise from the difference of the last two estimates in the VBS procedure and are therefore to be taken with care.

ψ	y	λ_c from (4.3)	$\Theta^{(1)}$	ν_x	$\nu_r = \nu_x\Theta^{(1)}$
0.1500	0.1511	$0.6855 \pm 1.1 \times 10^{-4}$	$0.9788 \pm 6.0 \times 10^{-4}$	$0.8432 \pm 2.5 \times 10^{-3}$	$0.8250 \pm 3.7 \times 10^{-3}$
0.3000	0.3093	$0.7436 \pm 3.4 \times 10^{-4}$	$0.8906 \pm 1.4 \times 10^{-3}$	$0.9062 \pm 1.5 \times 10^{-2}$	$0.8071 \pm 1.7 \times 10^{-2}$
0.4500	0.4830	$0.8399 \pm 1.4 \times 10^{-3}$	$0.7762 \pm 2.2 \times 10^{-3}$	$0.9508 \pm 8.0 \times 10^{-3}$	$0.7380 \pm 1.1 \times 10^{-2}$
0.5236	$1/\sqrt{3}$	$0.9034 \pm 3.2 \times 10^{-3}$	$0.7211 \pm 4.0 \times 10^{-3}$	$0.9660 \pm 1.2 \times 10^{-2}$	$0.6965 \pm 1.3 \times 10^{-2}$

The results of the finite-size scaling analysis are summarised in table 5 for the scaling of the correlation length and in table 6 for the scaling of the wavevector. Up

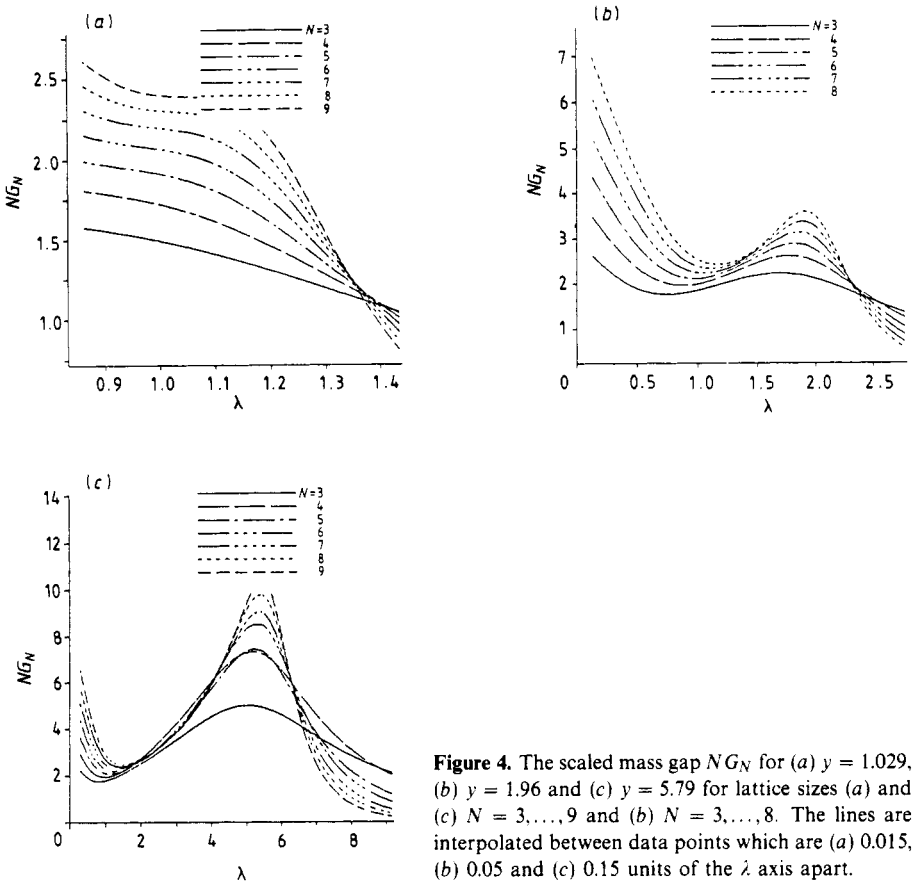

Figure 4. The scaled mass gap NG_N for (*a*) $y = 1.029$, (*b*) $y = 1.96$ and (*c*) $y = 5.79$ for lattice sizes (*a*) and (*c*) $N = 3,\ldots,9$ and (*b*) $N = 3,\ldots,8$. The lines are interpolated between data points which are (*a*) 0.015, (*b*) 0.05 and (*c*) 0.15 units of the λ axis apart.

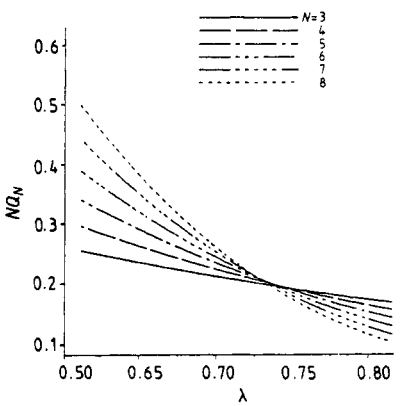

Figure 5. The scaled wavevector NQ_N for $y = 0.2027$ for lattice sizes $N = 3,\ldots,8$. The lines are interpolated between data points which were 0.015 units of the λ axis apart.

to $y \simeq 1/\sqrt{3}$ the correlation length scales at the same value of the coupling λ as the wavenumber which is also consistent with the series results of the previous section. The results check with those of Vescan *et al* (1986) at $y = 1/\sqrt{3}$ if one multiplies their

coupling constant λ by a factor of $(1 + y^2)$. The anisotropy parameter $\Theta^{(1)}$ decreases from the isotropic value 1 at $y = 0$ as y increases, indicating that the system is not conformally invariant in this region. The other anisotropy parameter $\Theta^{(2)}$ shows similar behaviour but starts off at a lower value.

Table 6. The extrapolated finite-size data following from the application of formulae (4.4), (4.5), (4.6*a*) and (4.6*b*). The system sizes considered were in the range $N = 3, \ldots, 10$. The finite-size estimates for the exponents and $\Theta^{(2)}$ were calculated at the extrapolated critical coupling λ_c. The indicated errors arise from the difference of the last two estimates in the VBS procedure and are therefore to be taken with care.

ψ	y	λ_c^{ferro} from (4.4)	$\Theta^{(2)}$	ν_x'	$\beta = \nu_x'\Theta^{(2)}$
0.1500	0.1511	$0.6854 \pm 1.0 \times 10^{-4}$	$0.7790 \pm 2.1 \times 10^{-3}$	$0.8185 \pm 1.7 \times 10^{-2}$	$0.6376 \pm 1.8 \times 10^{-2}$
0.3000	0.3093	$0.7429 \pm 2.8 \times 10^{-4}$	$0.7334 \pm 9.2 \times 10^{-4}$	$0.8393 \pm 4.5 \times 10^{-2}$	$0.6155 \pm 3.1 \times 10^{-2}$
0.4500	0.4830	$0.8380 \pm 1.9 \times 10^{-3}$	$0.6779 \pm 3.1 \times 10^{-4}$	$0.8837 \pm 4.5 \times 10^{-3}$	$0.5990 \pm 6.0 \times 10^{-2}$
0.5236	$1/\sqrt{3}$	$0.9030 \pm 1.2 \times 10^{-3}$	$0.6450 \pm 1.0 \times 10^{-3}$	$0.9008 \pm 4.1 \times 10^{-2}$	$0.5810 \pm 4.3 \times 10^{-2}$

The correlation length exponent ν_x rises regularly from the three-state Potts value $\nu_x = \nu_\tau = \frac{5}{6}$ at $y = 0$. With the help of $\Theta^{(1)}$ we can then calculate ν_τ and compare this with the series results. This fails the more the closer y is to the expected Lifshitz point around $y = 1/\sqrt{3}$. A similar discrepancy shows up if we compare ν_x with ν_x' which should be equal, because there should be only one critical length in the x direction. The last two findings do not depend on the extrapolation method used to obtain the exponents. We think this is an indication that finite-size scaling does not give reliable information around a Lifshitz point with the lattice sizes obtainable at the moment. Alternatively one could assume that the floating phase stretches out to $y = 0$ in a narrow strip and that this causes problems with the conventional scaling analysis. The behaviour of the wavenumber exponent $\overline{\beta}$, however, which monotonically decreases towards the Pokrovsky–Talapov value $\overline{\beta} = 0.5$ and which, for $y < 1/\sqrt{3}$, is consistently obtained both by the use of the high-temperature series and through finite-size scaling, points towards the existence of a Lifshitz point around $y = 1/\sqrt{3}$. This result is further substantiated by the appearance of loops in the mass gap around that value of y (see figures 4(*a–c*)).

4.2. The incommensurate floating phase

In the plots of the mass gap NG_N (see figures 4(*a–c*)) for $y > 1/\sqrt{3}$ the correlation length is seen to scale very nicely—especially for $y = 5.7979$—in an extended region of the coupling constant which increases rapidly as the chirality y increases. This scaling, which has not been found in earlier numerical studies of systems with competing interactions (Duxbury *et al* 1984, Domany and Schaub 1984, Beale *et al* 1985, Oitmaa *et al* 1987) clearly indicates a critical region and therefore the existence of a phase with algebraically decaying correlations. Just below the ferromagnetic phase transition line λ_c^{ferro} (see later) we note the appearance of a peak whose height increases with the size of the system. Thus it appears that the system mimics a paramagnetic phase between the ferromagnetic phase and the floating phase. This can be explained in the following way. The correlation length of the infinite system is infinite within the floating phase. Closely above the ferromagnetic domain boundary the density of walls is very low, i.e. the walls are very far apart. For a strip of finite width, however, the correlation length is finite and can—close to the ferromagnetic boundary—become smaller than the

average wall-to-wall distance. When this happens the results of a finite-size calculation will simulate a system of non-interacting domain walls and therefore show an artificial paramagnetic phase. If one increases the system size this effect will eventually saturate. We obtained further confirmation for this point of view by plotting NG_N for a constant value of the wavenumber Q, i.e. that we solved the equation $Q_N[y_N(\lambda), \lambda] = \text{constant}$ for a given system size N, then extrapolated the different curves $y_N(\lambda)$ to $y_\infty(\lambda)$ (figure 6) and calculated $G_N[y_\infty(\lambda), \lambda]$ (figure 7). Since the wall density for this case remains at a relatively high constant value, one never reaches the region where the peak in the mass gap appears. The rise in the value of the mass gap with increasing λ (see figures 4(*a–c*)) is caused by a temperature-dependent prefactor in front of the Hamiltonian (2.4) (see §5).

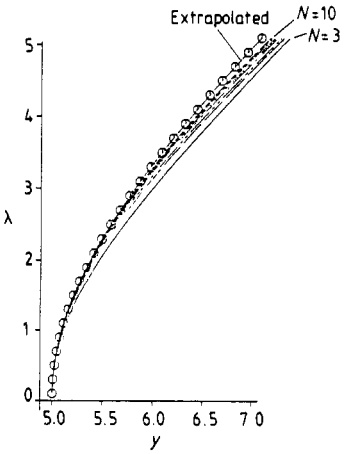

Figure 6. The curves $y_N(\lambda)$ for $Q = 5.0$ and for chain lengths $N = 3,\ldots,10$ and the extrapolated curve $y_\infty(\lambda)$.

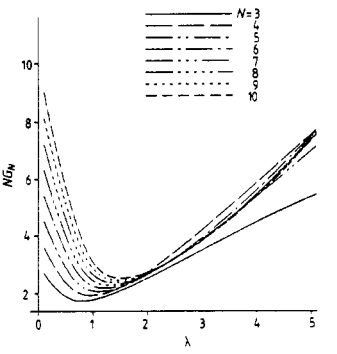

Figure 7. The scaled mass gap NG_N for $Q = 5.0$ for lattice sizes $N = 3,\ldots,10$. The lines are interpolated between data points taken at the extrapolated coordinates in the y–λ plane of figure 6.

In the previous paragraph we argued qualitatively for the existence of a floating phase through pictures of the scaled mass gap. We shall now assume that this phase is in fact a Kosterlitz–Thouless phase (Kosterlitz and Thouless 1973, Kosterlitz 1974) and shall try to verify this assumption by a finite-size scaling analysis. At criticality, i.e. at the melting line of the floating phase, the mass gap should thus develop an essential singularity of the form

$$G \sim \exp\left(\frac{\text{constant}}{(\lambda_c^{KT} - \lambda)^\sigma}\right) \qquad \lambda < \lambda_c^{KT}. \tag{4.8}$$

Introducing finite-size estimates λ_{cN}^{KT} for the critical coupling λ_c^{KT} we obtain for finite $N \gg 1$

$$G_N(\lambda) \simeq \exp\left(-\frac{\text{constant}}{[(\lambda_c^{KT} - \lambda_{cN}^{KT}) + (\lambda_{cN}^{KT} - \lambda)]^\sigma}\right) \qquad \lambda < \lambda_{cN}^{KT}. \tag{4.9}$$

Finite-size scaling implies that $G_N(\lambda_{cN}^{KT}) \simeq N^{-\Theta}$. Therefore we find from (4.9)

$$\lambda_c^{KT} - \lambda_{cN}^{KT} = \left(\frac{\text{constant}}{\Theta \ln N}\right)^{1/\sigma}. \tag{4.10}$$

The last two equations lead to a scaling form for the mass gap at the KT transition given by

$$G_N(\bar{\lambda}) \simeq N^{-\Theta}\hat{F}[(\ln N)^{1+1/\sigma}\bar{\lambda}] \qquad \bar{\lambda} = \lambda_{cN}^{KT} - \lambda > 0. \tag{4.11}$$

We take the minima of the mass gap as estimates for the finite-size critical couplings (see Hamer and Barber 1981) and perform a three-parameter fit to

$$\lambda_N^{\min} = \lambda_{cN}^{KT} = \lambda_c^{KT} - C_1/(\ln N)^{1/\sigma} \qquad N = 3, \ldots, 10 \tag{4.12}$$

for the parameters λ_c^{KT}, C_1 and σ. The results for λ_c^{KT} and σ for $y = 1.96$, $y = 5.79$ and $Q =$ constant $= 5.0$ are summarised in table 7 (for $y = 1.04$ the analysis could not be carried out since for system sizes up to $N = 9$ there is no minimum in the mass gap). The results for λ_c^{KT} are consistent with one another, i.e. λ_c^{KT} rises monotonically with increasing y. The exponent σ turns out to be independent of y and agrees with the KT value $\sigma = \frac{1}{2}$.

Table 7. The critical parameters of the melting transition from the modulated floating phase to the modulated paramagnetic phase. The indicated errors were obtained from the variation of the extrapolated values with the system sizes considered and are therefore rather subjective.

	λ_c^{KT}	σ
$\psi = 1.1$, $y = 1.96$	1.38 ± 0.20	0.499 ± 0.07
$Q = 5.0$, $y^{Q=5.0}(\lambda_c^{KT}) \simeq 5.4$	1.84 ± 0.19	0.558 ± 0.10
$\psi = 1.4$, $y = 5.7979$	1.96 ± 0.24	0.525 ± 0.12

5. Conformal invariance—the exponent η

The theory of the KT transition normally allows the conclusion that the system is conformally invariant in the KT phase, i.e. the classical fields have to satisfy the Laplace equation. The uniaxial oscillating factor in the correlation function (1.3) shows that the CC3 model—as it stands—is certainly not conformally invariant at criticality. The deviation of the anisotropy parameter Θ from unity that was previously observed for $y \leq 1/\sqrt{3}$ is a further sign that the model is not conformally invariant. On the other hand, for large values of y we do find a phase with algebraically decaying correlations over an extended regime of the coupling constant and a behaviour at the transition to the paramagnetic phase which agrees well with the predictions of KT theory. By plotting finite-size approximants Y_N to Θ (see figure 8) for $Q =$ constant $= 5.0$, where a wide KT phase exists, we notice that these fluctuate around unity within the KT phase. Thus for large values of y the concept of conformal invariance should be applicable to the CC3 model after a suitable modification has been made. Instead of the original spin variables (see (1.2)) one introduces the variables (Pokrovsky and Talapov 1978, 1980, Villain and Bak 1981)

$$S'(\boldsymbol{R}) = \exp\left[\mathrm{i}\left(\frac{2\pi}{3}n_{\boldsymbol{R}} - QR_\tau\right)\right] \tag{5.1}$$

in which the regular oscillations with wavenumber Q have been divided out so that their correlations decay monotonically.

$$\langle S'(\boldsymbol{R})S'(0)\rangle \simeq \frac{1}{R^{\eta}} \exp\left(-\frac{R_\tau}{\xi_\tau} - \frac{R_x}{\xi_x}\right). \tag{5.2}$$

Since, as we have found, scaling is isotropic in a certain area of the y–λ plane, i.e. $\xi_x \simeq \xi_\tau \simeq N$ for a strip of width N, we conclude that the CC3 model formulated in terms of the variables $S'(\boldsymbol{R})$ is conformally invariant in that area. This allows us to derive the exponent η in (5.2) and in (1.3) from finite-size approximants to the correlation length $\xi = G^{-1}$ (see e.g. Cardy 1987). The adopted procedure follows closely that derived by von Gehlen *et al* (1985).

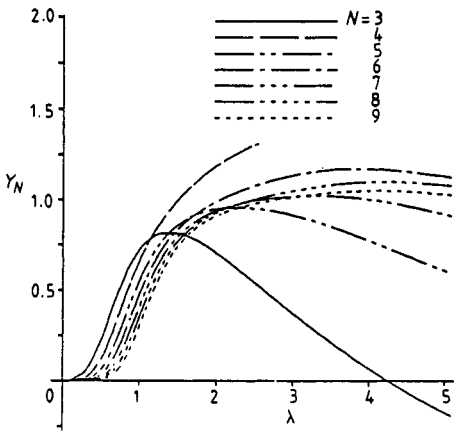

Figure 8. The function Y_N from formula (4.5) for constant wavevector $Q = 5.0$. The lines are interpolated between data points taken at the extrapolated coordinates in the y–λ plane of figure 6.

At the critical point in a conformally invariant system the mass gap G_N should directly give the order–disorder exponent η multiplied by a temperature-dependent prefactor $\epsilon(\lambda)$

$$\lim_{N\to\infty} NG_N = \pi\epsilon(\lambda)\eta. \tag{5.3}$$

The factor $\epsilon(\lambda)$ is given by (von Gehlen *et al* 1985)

$$\lim_{N\to\infty} N \operatorname{Re}\{\Lambda_N^{(1)}(1) - \Lambda_N^{(1)}(0)\} = 2\pi\epsilon(\lambda). \tag{5.4}$$

We did not use (5.4) to calculate $\epsilon(\lambda)$, because (5.4) was derived in the limit of large $\epsilon(\lambda)^2p^2/G^2$, so that

$$(G^2 + \epsilon(\lambda)^2p^2)^{1/2} \simeq \epsilon(\lambda)p \tag{5.5}$$

where p is the momentum, $p = 2\pi k/N$. Even for our largest systems ($N = 10$) this is not even approximately valid. Thus we used the unexpanded version of (5.4)

$$\lim_{N\to\infty} N\,[\operatorname{Re}\{\Lambda_N^{(1)}(1)\}^2 - \operatorname{Re}\{\Lambda_N^{(1)}(0)\}^2 - 2\Lambda_N^{(0)}(0)\operatorname{Re}\{\Lambda_N^{(1)}(1) - \Lambda_N^{(1)}(0)\}]^{1/2} = 2\pi\epsilon(\lambda). \tag{5.6}$$

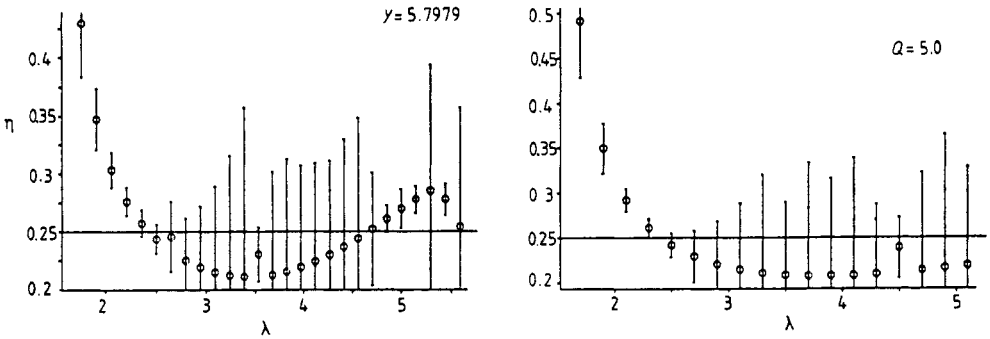

Figure 9. The exponent η as a function of λ given by conformal invariance as described in the text (*a*) for y=5.7979 and (*b*) for Q = constant = 5.0.

η was then calculated by extrapolating finite-size estimates of the ratio of (5.3) over (5.6).

In order to be able to predefine the convergence rate, we did not use VBS approximants but rather the method proposed by Bulirsch and Stoer (1964) (see also Henkel and Schütz 1988). The most consistent data were obtained with $\omega = 1$, i.e. that the finite-size estimates converged as $1/N$. The results for $y = 5.79$ and for Q = constant = 5.0 are shown in figures 9(*a*) and (*b*). The error bars were obtained as the difference between the last BS estimate and the BS estimate of the second last generation. The large error bars in the regime of the floating phase arise from the fact that the finite-size data are still relatively far apart for the system sizes we could obtain. The extrapolation was further obstructed by an even–odd asymmetry (see also figure 4(*c*) for NG_N and figure 8 for Θ), which arises from similar excitations for the quantum chain for the corresponding even–odd pair. In spite of all these difficulties in the extrapolation procedure we think that the continuous behaviour of the extrapolated values gives rise to some confidence in their quantitative behaviour. Both parts of figure 9 show a decrease in the value of η to a minimal value of around 2/9 which agrees with the predicted value $2/q^2$ (Schulz 1980, 1983, Ostlund 1981, Haldane *et al* 1983) where q is the number of spin states. For $y = 5.79$, η rises again for increasing values of the coupling constant, whereas for the Q = constant case η seems to remain rather constant. This difference is probably due to the finite-size effects (see above) close to the ferromagnetic phase boundary. From the line $\eta(\lambda) = \frac{1}{4}$ we were able to obtain guesses for the value of the coupling constant at the KT transition. These turned out consistently higher than the values of the critical coupling obtained from finite-size scaling (see table 7). We explain this discrepancy by the difficulty of fitting finite-size data to a logarithmic scaling law with a high degree of accuracy.

6. Summary

We have shown that the transfer matrix of the two-dimensional chiral clock model can be represented as the exponential of a one-dimensional non-Hermitian quantum Hamiltonian. The parameter that controls the non-Hermiticity of the quantum Hamiltonian corresponds to the chirality parameter of the original model. The derivation of the Hamiltonian suggests that for small chirality, $y \leq 1/\sqrt{3}$, there is a direct phase transition from the spatially modulated disordered phase to the ferromagnetic phase of

the chiral clock model. For large chirality an incommensurate floating phase intervenes between these two phases.

For $y \leq 1/\sqrt{3}$ we determined the critical coupling λ_c, the critical exponents ν_x and ν_τ of the correlation lengths ξ_x and ξ_τ along the two lattice directions and the critical exponent $\overline{\beta}$ of the wavevector Q of the modulation of the disordered phase. This has been done by considering a series expansion of the eigenvalues of the Hamiltonian and by finite-size scaling. From finite-size scaling we find that for $y \leq 1/\sqrt{3}$ the correlation lengths and the wavenumber scale at the same coupling λ_c. This agrees with the suggestion that there be only one phase transition in this range of chirality. Within the achieved accuracy the two techniques yield identical values for $\overline{\beta}$, which varies from $\overline{\beta} \simeq 0.65$ for $y = 0.1511$ to $\overline{\beta} \simeq 0.57$ for $y = 1/\sqrt{3}$. According to finite-size scaling the system scales anisotropically for any finite chirality $y \leq 1/\sqrt{3}$. The anisotropy $\Theta^{(1)} = \nu_\tau/\nu_x$ develops continuously as y increases and reaches a value of about 0.72 at $y = 1/\sqrt{3}$. Howes (1983), who argued for a Lifshitz point at finite chirality, conjectured that the correlation length exponents take the values $\nu_x = 1$, $\nu_\tau = \frac{2}{3}$ at that point. Our values at $y = 1/\sqrt{3}$, $\nu_x \simeq 0.97$, $\nu_\tau \simeq 0.7$, compare favourably with this conjecture. From the series expansion, however, we find a different behaviour of ν_τ. Also the values obtained for ν_x from correlation length scaling and from wavevector scaling differ significantly. Thus, in our opinion, the possibility that the floating phase extends to $y = 0$ in a very narrow strip between the disordered and the ferromagnetic phase, i.e. that there is no Lifshitz point for a finite chirality, cannot definitely be ruled out.

For $y > 1/\sqrt{3}$ we find clear evidence for the occurrence of an incommensurate floating phase: the mass gap scales isotropically in an extended region of the phase diagram. The loop structure in the scaling function Y_N which has previously been interpreted as a qualitative indication for such a phase is presumably induced by finite-size effects which artificially make the wavelength of the modulation longer than the correlation length for the finite system. Conventional finite-size scaling analysis, which relies on the scaling of a critical property of the system at one single value of the coupling, fails here due the existence of an extended critical region containing the floating phase. An appropriate finite-size scaling analysis, however, confirms that the melting of the floating phase occurs via a Kosterlitz–Thouless transition. At the transition to the ferromagnetic phase the wavevector of the modulation of the floating phase is found to vanish with a critical exponent $\overline{\beta} = 0.5$ as predicted by Pokrovsky and Talapov (1978, 1980).

The isotropic scaling of ξ in a finite region of the y–λ plane suggests that the model should be conformally invariant when formulated in appropriately defined new spin variables. Exploiting the consequences of conformal invariance we extracted the critical exponent η from finite-size approximants of the mass gap of the Hamiltonian. The results are consistent with our view that the floating phase of the chiral clock model is a Kosterlitz–Thouless phase.

Acknowledgments

One of the authors (HUE) thanks the Max-Planck-Institut für Festkörperforschung in Stuttgart and the Institut für Festkörperforschung der KFA Jülich for their hospitality. During visits at these institutes the series expansion was worked out. We wish to thank V Rittenberg whose comments led to the development of §5. The numerical calculations were carried out at the Regionales Rechenzentrum für Niedersachsen, Hannover.

References

Barber M N 1983 *Phase Transitions and Critical Phenomena* vol 8, ed C Domb and J L Lebowitz (New York: Academic) pp 145–266

Beale P D, Duxbury P M and Yeomans J M 1985 *Phys. Rev.* B **31** 7166

Bulirsch R and Stoer J 1964 *Num. Math.* **6** 413

Cardy J L 1987 *Phase Transitions and Critical Phenomena* vol 11, ed C Domb and J L Lebowitz (New York: Academic) pp 55–126

Centen P, Rittenberg V and Marcu M 1982 *Nucl. Phys.* B **205** 585

Cullum J K and Willoughby R A 1985 *Lanczos Algorithms for Large Scale Symmetric Eigenvalue Computations* vol 1 *Theory*, vol 2 *Programs* (Basel: Birkhäuser)

——1986 *Large Scale Eigenvalue Problems* (*Mathematical Studies* **127**) ed J K Cullum and R A Willoughby (Amsterdam: North Holland)

Domany E and Schaub B 1984 *Phys. Rev.* B **29** 4095

Duxbury P M, Yeomans J and Beale P D 1984 *J. Phys. A: Math. Gen.* **17** L179

Elizur S, Pearson R B and Shigemitsu J 1979 *Phys. Rev.* D **19** 3698

Haldane F D M, Bak P and Bohr T 1983 *Phys. Rev.* B **28** 2743

Hamer C J and Barber M N 1981 *J. Phys. A: Math. Gen.* **14** 2009

Hamer C J, Kogut J B and Susskind L 1979 *Phys. Rev.* D **19** 3091

Henkel M and Schütz G 1988 *J. Phys. A: Math. Gen.* **21** 2617

Houlrik J M, Knak Jensen S J and Bak P 1983 *Phys. Rev.* B **28** 2883

Howes S F 1983 *Phys. Rev.* B **27** 1762

Huse D A 1981 *Phys. Rev.* B **24** 5180

Huse D A and Fisher M E 1982 *Phys. Rev. Lett* **49** 793

——1984 *Phys. Rev.* B **29** 239

Imbihl R J, Behm J, Christmann K, Ertl G and Matsushima J 1982 *Surf. Sci.* **117** 257

Kadanoff L P and Kohmoto J 1981 *J. Phys. A: Math. Gen.* **14** 1291

Kinzel W and Yeomans J M 1981 *J. Phys. A: Math. Gen.* **14** L163

Kogut J B 1979 *Rev. Mod. Phys.* **51** 659

Kosterlitz J M 1974 *J. Phys. C: Solid State Phys.* **7** 1046

Kosterlitz J M and Thouless D J 1973 *J. Phys. C: Solid State Phys.* **6** 1181

Lanczos C 1950 *J. Res. NBS* **45** 255

Marcu M, Regev A and Rittenberg V 1981 *J. Math. Phys.* **22** 2740

Nightingale M P 1976 *Physica* **83A** 561

Oitmaa J, Batchelor T M and Barber M N 1987 *J. Phys. A: Math. Gen.* **20** 1507

Ostlund S 1981 *Phys. Rev.* B **24** 398

Paige C C 1972 *J. Inst. Maths. Appl.* **10** 373

Pokrovsky V L and Talapov A L 1978 *Sov. Phys.-JETP* **48** 579

——1980 *Sov. Phys.-JETP* **51** 134

Schaub B and Domany E 1983 *Phys. Rev.* B **28** 2897

Schulz H J 1980 *Phys. Rev.* B **22** 5274

——1983 *Phys. Rev.* B **28** 2746

Selke W and Yeomans J M 1982 *Z. Phys.* B **46** 311

Van den Broeck J M and Schwartz L W 1979 *SIAM J. Math. Anal.* **120** 658

Vescan T, Rittenberg V and von Gehlen G 1986 *J. Phys. A: Math. Gen.* **19** 1957

von Gehlen G, Rittenberg V and Ruegg H 1985 *J. Phys. A: Math. Gen.* **19** 107

Villain J and Bak P 1981 *J. Physique* **42** 657